Effect of interlaying UV-irradiated PEEK fibres on the mechanical, impact and fracture response of aerospace-grade carbon fibre/epoxy composites

Quan, Dong; Deegan, Brian; Binsfeld, Lucas; Li, Xiping; Atkinson, Jason; Ivanković, Alojz; Murphy, Neal

DOI
10.1016/j.compositesb.2020.107923

Publication date
2020

Document Version
Accepted author manuscript

Published in
Composites Part B: Engineering

Effect of interlaying UV-irradiated PEEK fibres on the mechanical, impact and fracture response of aerospace-grade carbon fibre/epoxy composites

Dong Quan[a], Brian Deegan[b], Lucas Binsfeld[c], Xiping Li[d], Jason Atkinson[c], Alojz Ivanković[c], Neal Murphy[c,*]

[a]*Structural Integrity & Composites Group, Faculty of Aerospace Engineering, Delft University of Technology, Netherlands*
[b]*Adhesives Research, Henkel Ireland Operations & Research Ltd., Ireland.*
[c]*School of Mechanical and Materials Engineering,University College Dublin, Ireland*
[d]*College of Engineering, Zhejiang Normal University, China*

Abstract

Poly-etherether-ketone (PEEK) fibres (average diameter 30 μm) were surface-activated by a UV-irradiation technique, and then used as interlayers of carbon fibre/epoxy composites. The results of a flatwise tensile test demonstrated a significant improvement in the PEEK fibre/epoxy adhesion upon the UV-treatment, i.e. the ultimate strength increased from 0.6-0.7 MPa to 7.6 MPa. Accordingly, interlaying UV-irradiated PEEK fibres resulted in considerable increases in the maximum values of open-hole tensile strength, Charpy impact strength and mode-I fracture energy, i.e. of 12 %, 131 % and 293 %, respectively. However, it also decreased the flexural strength by 29 %, owing to the thickness increase caused by adding interlayers. Fortunately, the load carrying capacity (the maximum failure load under flexural bending) was largely unaffected, and moreover, an average residual strength of 475$\pm$23 MPa still remained after the damage at the maximum load. The results demonstrated significant benefits of using longitudinal UV-irradiated PEEK fibres as interlayers of CFRPs.

Keywords: A: Polymer-matrix composites (PMCs), PEEK-fibre interlayers, B:

*Corresponding author. Tel: +353 (1) 7161940; Email: neal.murphy@ucd.ie (Neal Murphy)

Delamination, D: Mechanical testing, E: Surface treatment.

1. Introduction

Fibre reinforced plastics (FRPs) are replacing traditional metals for various applications due to their high strength-to-weight ratio and excellent structural performance. Nevertheless, the laminated structure of FRPs results in inherently low interlaminar properties, and hence poor resistance to impact damage and crack propagation. This restricts a wider application of the FRPs. Therefore, enhancing the interlaminar properties, especially the impact resistance and fracture toughness, of FRPs has been a research focus over the last two decades. A number of strategies have been proposed for the interlaminar enhancement of FRPs, including adding second-phase modifiers into the epoxy matrix [1–4], introducing reinforcement features in the through thickness-direction by 3D-textile weaving [5, 6], Z-pinning [7, 8], and stitching [9], and interlaying different materials between the plies of the carbon fibre fabrics [10–13]. While different levels of success in terms of interlaminar enhancement have been achieved, there are also some issues associated with different methods. For example, the presence of second-phase modifiers in the epoxy matrix will notably decrease its flowability [4, 14, 15], and subsequently increase the difficulties for laminate manufacturing, especially for the infusion-based manufacturing methods. The use of 3D weaving, Z-pinning and stitching methodologies can lead to deteriorations in the in-plane mechanical properties [9, 16, 17]. Moreover, the toughening performance of Z-pinning and stitching was found to be dependent on the laminate stacking sequence [18, 19], e.g. Francesconi and Aymerich [19] revealed that Z-pinning had no significant effects on the impact performance of $[0_2/\pm45]_s$ and $[0/\pm45/90]_s$ laminates. Among different strategies, interlay-toughening is an easy method that does not necessarily increase manufacturing cost. In general, any material can be simply placed between the plies of the FRPs, and hence, it offers researchers the flexibility to tailor the mechanical, fracture and impact properties of the laminates by using different types and amounts of interlayers. Accordingly, it is attracting considerable attention

from both academic researchers and industrial engineers.

Various materials, such as carbon nanotubes (CNTs) or carbon nanofibres (CNFs) [20–23], graphene [24, 25], metal fibres [10], hybrid CNTs/short fibres [26, 27] and thermoplastic phases [28–30], have been used as interlayers to toughen FRPs. Interlay toughening is generally accepted to be promising for the interlaminar enhancement of FRPs. For example, Zhou et al. [26] used 1 mg/cm^2 hierarchical carbon nanotube-short carbon fiber (CNT-SCF) as interlayers of a carbon fibre/epoxy laminate and reported an improvement of 125 % in the mode-I fracture energy (G_{IC}). Similarly, G_{IC} increased by 326 % [31] and 100 % [20], respectively upon interlaying 10 g/m^2 PA veils to carbon fibre reinforced plastics (CFRPs). Regarding impact performance, an improvement of 37 % in the impact absorption energy was obtained by interlaying 1 wt.% glass nanofiber mats to glass fibre reinforced plastics (GFRPs) [32]. In another study, it was reported that the Charpy impact strength of a CFRP was increased by 18 % upon interlaying 1.05 g/m^2 PA66 veils [33]. It should be noted that opposite influences on the other mechanical properties upon interlaying have been observed in different publications, e.g. the flexural modulus and strength of CFRPs remained unchanged or were even improved by interleaving thermoplastic nonwovens in some studies [33–37], while an opposite trend was observed in other literature [29, 38, 39]. The different toughening levels and varying effects on the mechanical properties can be linked to many factors, including the adhesion between the epoxy matrix and the interlayers, the mechanical properties of the interlayers, the architecture of the carbon fibre fabrics and the quantity of interlayers employed (which subsequently affects the volume fraction of the carbon fibres in the interleaved laminates).

Poly-etherether-ketone (PEEK) is a high-performance, engineering thermoplastic characterised by an exclusive combination of properties, including exceptional mechanical properties, excellent long-term chemical resistance and high temperature resistance. It is an attractive candidate as an interlayer material for toughening FRPs. However, the number of studies on the use of PEEK for this purpose is limited. Ramirez et al. [40] employed a PEEK nonwoven veil with an areal density of 10 g/m^2 as interlayers of unidirectional CFRPs, and

observed an increase of approximately 100 % and 320 % for G_{IC} and mode-II fracture energy (G_{IIC}), respectively. To the best knowledge of the authors, there is still no systematic study on the mechanical, fracture and impact performance of FRPs interleaved with PEEK based materials. One of the main restrictions for using PEEK as interlayers of carbon fibre/epoxy composites is the poor PEEK/epoxy interface adhesion, as a result of the low polar surface energy of PEEK. This will negatively affect not only the toughening performance of the PEEK interlayers, but also the other mechanical properties of the laminates. Herein, an easy and effective UV-irradiation method has been proposed to treat the surfaces of PEEK fibres (of average diameter 30 μm) to significantly improve the PEEK/epoxy adhesion. The UV-irradiated PEEK fibres were then used as interlayers of a carbon fibre/epoxy composite, with an attempt to enhance the mechanical, fracture and impact performance. The flexural strength, open-hole tensile strength, Charpy impact strength and fracture toughness of the interleaved laminates were studied, and the corresponding failure mechanisms were investigated.

2. Experimental

2.1. Materials and sample preparation

The 5-Harness satin weave (5H) carbon fibre/epoxy prepreg consisting of AS4 carbon fibres was Hexply 8552/5H from Hexcel, UK. The areal density and fibre volume fraction of the prepreg were 615 g/m^2 and 55 %, respectively. The unidirectional (UD) carbon-fibre/epoxy prepreg based on T300 carbon fibres was HYE 1034E from Cytec, Solvay Group. It possessed an areal density of 230 g/m^2 and a carbon fibre volume fraction of 57-63 %. The PEEK fibres (multifilament, 1230f72) were supplied by Zyex, UK in the form of a continuous bundle. The bundle contains 72 filaments, which have an average diameter of 30 μm. A photo of the PEEK fibre yarn and a typical microscopy image of a PEEK fibre are shown in Figure 1.

The PEEK fibres were manually wound onto a piece of cardboard with a target areal density of 100 g/m^2, as shown in Figure 1 (a). To ensure the areal density of the PEEK fibres was uniform within one layer and repeatable between different layers, the following procedure was followed. Cardboard sheets of the same dimensions of 200 mm$\times$200 mm were used to form simple bobbins, and the PEEK fibres were wound onto a pre-marked region of the cardboard with an area of 200 mm$\times$150 mm. The weight increase during the winding was regularly monitored for every coverage area of 200 mm$\times$10 mm to ensure a local areal density of 100$\pm$5 g/m^2 was obtained. The final areal density of the PEEK fibres on each cardboard sheet was calculated based on the weight of the PEEK fibres divided by the coverage area. In total, 20 sheets of cardboard wound with PEEK fibres were prepared and an areal density of 98$\pm$4 g/m^2 was obtained in every case. The PEEK/cardboard bobbin was then placed in an in-house UV-irradiation system in Henkel (Ireland) for surface treatment, aiming to improve the adhesion between the PEEK fibres and the carbon fibre prepreg. The UV-irradiation system was equipped with a Light Hammer 6 UV source, from Heraeus Noblelight, UK. The PEEK fibres were placed 25 cm below the UV lamp for a 60 s treatment. The intensities of the UV spectral ranges were determined using a UV Power Puck from EIT Inc., USA [41]. The UV Power Punk was placed at the same distance from the source, facing the UV light during the measurement. The intensities of UVV (395-445 nm), UVA (320-390 nm), UVB (280-320 nm) and UVC (250-260 nm) were found to be 371 mW/cm^2, 414 mW/cm^2, 141 mW/cm^2 and 23 mW/cm^2, respectively. After the PEEK fibres facing the UV lamp were treated, the cardboard was inverted to continue with the treatment of the fibres on the opposite side. A number of PEEK rods (the same grade of PEEK as the fibres) with a cross sectional diameter of 12.7 mm were also surface activated using the UV light by following the same procedure. They were used for surface characterisation of the UV-treated PEEK polymer, as well as for a flatwise tensile test to qualitatively evaluate the effects of the UV-irradiation on the adhesion at the carbon fibre prepreg/PEEK interface. A mobile surface analyser from KRÜSS, GmbH. was used to measure the surface free energies and water contact angles of the UV-treated

and non-treated PEEK rods. The chemical composition on the PEEK surface before and after UV-irradiation was studied using a X-Ray photoelectron spectrometer (XPS, Kratos Axis Ultra DLD), equipped with an Al-Kα (1486.7 eV) X-ray source.

A layup consisting of 8 layers of 5H prepregs and 7 layers of PEEK fibres was prepared to manufacture the laminates interleaved with PEEK fibres between every ply. To manufacture the specimens for the fracture tests, only one layer of PEEK fibres was incorporated at the mid-plane of the laminates. In this case, 14 plies of 5H prepregs or 26 plies of UD prepregs with one layer of PEEK fibres at the mid-plane were stacked together to make the layups. The detailed procedure for transforming the PEEK fibres from the cardboard sheets to the carbon fibre prepreg is schematically shown in Figure 2. In step 1, a strip of tacky tape was placed and pressed onto one edge of the PEEK fibres to tightly stick the PEEK fibres onto the cardboard sheet. The PEEK/cardboard bobbin was then firmly pressed onto the prepreg. Since the carbon fibre prepreg was very sticky due to the presence of non-cured epoxy, all the PEEK fibres at the bottom surface of the cardboard adhered well to the prepreg. In step 2, the left edge of the bobbin was firstly cut off using a scissors following the black dashed line in Figure 2. After that, the bobbin was flipped, gently stretched and then firmly pressed down onto the prepreg. It should be noted that the tacky tape held the PEEK fibres well onto the cardboard during the stretching, that ensured no distortion of the PEEK fibres. Finally, the cardboard sheet and the tacky tape were removed by chopping the cardboard following the black dashed line in step 3 in Figure 2. A PTFE insert (with a thickness of 12.5 μm) was also placed at the mid-plane of the laminates during the layup procedure, to create the crack starter for the fracture test specimens. The layups were then cured inside an in-house pressclave under vacuum with an internal pressure of 80 psi (5.5$\pm$0.2 bar) applied in the mould chamber. The cure cycle consisted of a 2-hour linear ramp from room temperature to 180 °C followed by a 2-hour dwell at 180 °C. The thickness of the control laminate without PEEK fibres based on 8 layers of 5H prepregs was measured to be 3.1 mm. The addition of 7 layers of PEEK fibres increased the thickness of the laminate to 3.6 mm for both the

non-treated and UV-treated PEEK fibres. The final thickness of the UD laminate consisting of 26 plies of UD prepregs and the 5H laminate based on 14 plies of 5H prepregs was measured to be 3.9 mm and 5.2 mm, respectively. The addition of one layer of PEEK fibres at the mid-plane had no obvious effect on the thickness. Figure 3 shows representative optical microscopy images of the 5H laminates with and without PEEK fibres between all the plies, showing no visible voids between the plies due to the incorporation of the PEEK fibres. It should be noted that the thickness of the PEEK fibres along the length direction appeared non-uniform in Figure 3, owing to the 5-Harness satin weaving style of the carbon fibre fabrics. The standard deviations of measurements for the laminate thickness were within 0.1 mm for all the cases, based on 20 measurements at different locations of a laminate panel of dimensions 300 mm$\times$500 mm. This indicates that the homogeneity of the PEEK fibre layers was reasonably good.

Figure 4 (a) presents a schematic of the flatwise tensile test specimens. To prepare these specimens, a bonding rig was designed to ensure the concentric and parallel alignment of the PEEK rods. A schematic of the lower section of the bonding rig is shown in Figure 4 (b). Three PEEK rods were secured into the nesting holes of each section of the rig before the application of a layer of the carbon fibre/epoxy prepreg. The two halves of the bonding rig were then assembled together under the guidance of two hardened aligning rods to form a joint. The assembled rig was then clamped with two large spring clamps, which applied a pressure of 80$\pm$3 psi on each PEEK rod joint. The assembled joints were finally placed in an air-circulated oven for curing with the same temperature schedule as for the laminate curing.

2.2. Test procedure

Three replicate tests were conducted for the flatwise tensile test at a loading rate of 1 mm/min. A three-point bend flexural test was carried out to determine the flexural strength of the laminates according to ISO14125 [42]. The width and length of the samples were 15 mm and 200 mm, respectively. The test was performed at a loading rate of 5 mm/min

with a supporting span of 160 mm. The diameter of the loading and supporting pins was 5 mm. Three samples were tested for each case. An open-hole tensile (OHT) test was performed to measure the failure strength of the laminates by following ASTM-D5766 [43]. The samples had a width of 25 mm and a length of 250 mm, and the diameter of the hole in the centre of the samples was 5 mm. The holes were drilled with a diamond film coated drill for aerospace composites from LMT Onsrud, USA. During drilling, the composite plates were backed with wood to minimize fraying and delamination during tool entry and exit. The test was performed at a loading rate of 1 mm/min, and was repeated on 5 samples for each case. During the OHT test, a LaVision DIC system (Davis10 software) equipped with two Imager M-lite 5M cameras was used to monitor the full-field strain distribution around the hole. A Charpy impact test according to ISO179-1 [44] was carried out on a XC-22D impact tester (from VTS, China), providing an impact speed of 3.5 m/s^2 and a stored energy of 22 J. A flatwise impact test with a normal blow direction was performed on unnotched specimens with a width of 15 mm, a length of 100 mm, and a supporting span of 40 mm. Eight samples were tested for each set. The mode-I fracture performance of the laminates was studied using a double cantilever beam (DCB) test according to ISO15024 [45]. A corrected beam theory was used to calculate the mode-I fracture energy of the DCB specimens. The length and width of the DCB specimens were 190 mm and 20 mm, respectively, with a 65 mm long crack starter. A 5 mm long precrack was generated by loading the samples under an opening mode. The DCB tests were then conducted at a constant displacement rate of 2 mm/min. In this work, the crack initiation values for G_{IC} were determined using the 5% offset approach, as described in the standard [45]. At least three replicate tests were conducted for the DCB tests. The flatwise tensile, three-point bend and DCB tests were performed on a screw-driven Hounsfield H50KS testing machine, and the OHT test was carried out on an Instron 5982 testing machine. It should be noted that the orientation of the PEEK fibres was longitudinal to the length of the specimens for the flexural, OHT and Charpy impact tests, and was either longitudinal or transverse to the crack propagation direction of the DCB specimens.

3. Results and Discussion

3.1. Surface characterisation

Table 1 shows the amount of carbon and oxygen elements, surface free energies and water contact angles of the surfaces of the UV-treated and non-treated PEEK rods. It should be noted that PEEK (Origin) means the original PEEK, and PEEK (UV) is the UV-irradiated one. It was observed that the amount of carbon element decreased from 82.29 % for the non-treated PEEK to 73.44 % for the UV-treated one, while the amount of oxygen element increased from 14.55 % to 22.02 %. This was due to the breakage of the C-C/C-H species and subsequent oxidation reactions, which generated additional C-O and C=O species and also developed new O-C=O species [46–48], as shown in Figure 5. The UV-irradiation had negligible effects on the total surface free energy (γ), and a value of around 50 mN/m was measured for both the control PEEK and UV-irradiated PEEK, as shown in Table 1. However, it was found that the polar component of the surface free energy (γ_s) considerably increased from 1.71 mN/m to 6.61 mN/m upon the UV-irradiation, corresponding to an essentially equivalent decrease in the dispersive component (γ_d). At the interface of two phases, the dispersive force is responsible for the temporary fluctuations of the charge distribution in the atoms/molecules, such as the van der Waals interactions, and the polar force generates Coulomb interactions between permanent dipoles and between permanent and induced dipoles, e.g. hydrogen bonds. Hence, a higher polar force is promising to obtain a stronger bond. The effects of UV-irradiation on the surface chemical composition and surface free energies resulted in considerably improved wettability of the PEEK surface, i.e. the water contact angle decreased from 81.49 ° to 69.09 °. All these observations, i.e. more oxidation groups, higher surface polar force and better wettability of the PEEK surface upon the UV-irradiation significantly improved the adhesion between the PEEK and the carbon fibre prepreg. Figure 6 (a) presents the ultimate strengths of the flatwise tensile specimens. It was found that the UV-irradiation significantly increased the ultimate strength from 0.6-0.7 MPa for the non-treated PEEK joints to 4.9 MPa for the UD prepreg bonded joints, and further to

7.6 MPa for the 5H prepreg bonded joints. Typical photos of the failure surfaces of the flatwise tensile specimens are presented in Figure 6 (b). Interfacial failure between the prepreg and the PEEK rods took place for the non-treated joints, leaving a clear surface on one side of the PEEK rods. The UV-irradiation resulted in cohesive failure inside the UD and 5H preprepg, evidenced by the presence of carbon fibres on both sides of the PEEK rods. In conclusion, the results of the flatwise tensile test qualitatively demonstrated significant increases in the PEEK/epoxy adhesion by the UV-irradiation treatment on the PEEK surface.

3.2. Flexural test

Figure 7 shows the results of the three-point bend flexural tests of the 5H laminates interleaved with and without PEEK fibres between all the plies. The incorporation of original PEEK fibres to the 5H laminates resulted in a considerable drop in the maximum load and corresponding displacement, as shown in Figure 7 (a). This corresponded to a significant decrease in the flexural strength from 1209 MPa to 486 MPa (see Figure 7 (b)). The flexural strength of the interleaved laminates notably increased from 486 MPa to 855 MPa upon application of the UV-irradiation to the PEEK fibres. Even though this value was still 29.3 % lower than that of the control laminate, the maximum load on the load-displacement curves of the laminates interleaved with UV-irradiated PEEK fibres was more or less the same as that of the control laminate, as can be seen in Figure 7 (a). The decrease in the flexural strength was due to the thickness increase of the laminates by adding interlayers. Moreover, the control laminate failed completely once the maximum load was reached (the load dropped to zero), while the PEEK fibre interleaved laminates still possessed some load carrying capacity at the same stage, i.e. an average value of 398 N for the specimens containing UV-treated PEEK fibres. The results of this study agreed well with the observations in the literature [33, 36, 49], i.e. the effects of interlaying on the flexural properties of CFRPs are closely linked to the adhesion between the interlayers and the epoxy matrix. It is well known that the flexural properties of CFRPs are dominated by the carbon fibre reinforcements. A

poor interlayer/epoxy adhesion adversely affects the load-transfer capacity between adjacent carbon fibre plies, and subsequently causes a decrease in the flexural properties. In contrast, an improved adhesion between the interlayers and the epoxy matrix should improve load transfer, and hence enhance the utilisation of the carbon fibres. Figure 8 shows the failure modes of the flexural test specimens for different laminates. The microscopy images in Figure 8 (b), focused on the damage region of the fracture samples, were taken by a KEYENCE laser scanning microscope (VK-X1100). It was found that, instead of breaking at the loading point (as observed for the control laminate), an upward bulge, i.e. out-of-plane bulking, occurred on the top side of the specimens beside the loading pin (as shown by the insert image in Figure 8 (a)) for all the interleaved laminates. This was due to the separation of the carbon fibre plies under a compression stress in the direction along the length of the samples. Figure 8 (b) shows typical microscopy images of the failure section of the flexural specimens. It was observed that the control laminate completely broke into two halves at the loading point, with relatively small amount of inter-ply delaminataion in the vicinity of the fracture point. For the original PEEK fibre interleaved laminates, inter-ply separation took place between all the top six plies of adjacent carbon fibres, with no visible carbon fibre breakage at this scale. This can also be clearly seen in the insert image of Figure 8 (a). This phenomenon was due to the poor adhesion between the PEEK fibres and the carbon fibre plies, in which case, the delamination relieved the stress concentration/accumulated energy, and subsequently prevented severe damage to the carbon fibres. An improved PEEK/epoxy adhesion upon UV-irradiation obviously changed the failure mode of the interleaved laminates, i.e. the level of inter-ply separation significantly dropped, and a number of carbon fibre plies delaminated and broke during the failure process.

3.3. Open-hole tensile (OHT) test

The load versus displacement curves of the OHT test are summarised in Figure 9 (a). It was observed that all the curves consisted of two linear sections those were connected with

a non-linear transition region. The cross points on the curves indicate the initiation of the transition region or 'kink', after which, the damage started and the stiffness of the specimens significantly dropped. The addition of PEEK fibres significantly increased the kink load and the ultimate load of the specimens, i.e. the kink load increased from 14.3 kN for the control laminate to 19.9 kN (by 39 %) and 20.7 kN (by 45 %) for the laminates interleaved with original and UV-treated PEEK fibres, respectively, and the ultimate load correspondingly increased from 27.9 kN to 35.9 kN (by 28.7 %) and 36.7 kN (by 31.6 %). This resulted in subsequent increases in the kink strength and the ultimate strength of the laminates, as shown in Figure 9 (b). However, the percentage increases in the strength were less prominent than those of the load owing to the thickness increase upon interlaying, i.e. an increase of 9.7 % and 12.2 % in the ultimate strength was observed for interlaying the original and UV-treated PEEK fibres, respectively. Figure 10 shows the full-field engineering von Mises equivalent strain (ε_{vM}) contours of the surfaces of the OHT specimens at the time of the kink and at the instant before the failure. More or less the same strain distribution was observed in all cases. However, the values of the maximum strain corresponding to the kink and failure of the specimens significantly increased due to the addition of the PEEK fibres.

The improvements in the damage tolerance of the CFRPs upon interlaying PEEK fibres can be explained by its effects on the failure mechanisms. Figure 11 shows typical images of the fractured OHT specimens, and the bottom images are the side-view in the vicinity of the fracture plane. It was found that the fracture took place at the mid-plane of the specimen for the control laminate, leaving a relatively clean and flat fracture surface across the width of the specimen. Moreover, no visible inter-ply separation was observed from the side-view images of the control laminate. This indicates a typical brittle failure mechanism of the control laminate [50, 51]. Unlike the control laminate, a carbon fibre pull-out mechanism was observed for the laminates interleaved with original and UV-treated PEEK fibres, and more over, the side-view images show evidence of extensive carbon fibre inter-ply separation in the vicinity of the fracture plane. The pull-out of carbon fibres was caused by carbon fibre

delamination, off-axis ply-cracking and carbon fibre splitting [50]. This, together with the additional pull-out and breakage of PEEK fibres, as shown in Figure 11, relieved the stress concentration around the hole, and subsequently led to the improvements in the OHT strength of the laminate.

3.4. Charpy impact test

The Charpy impact strengths of the laminates are summarised in Figure 12 (a). It was found that the impact strength of the 5H laminate increased from 80.8 kJ/m^2 for the control laminate to 129.5 kJ/m^2 (by 60 %) by interlaying the original PEEK fibres, and further to 187.0 kJ/m^2 (by 131 %) by adding the UV-irradiated PEEK fibres. Figure 12 (b) presents typical photographs of the tested impact specimens, showing different failure modes in different cases. For the control laminate, the specimens were completely separated into two halves due to the impact. Inter-ply delamination between all the carbon fibre plies dominated the failure of the original PEEK fibre interleaved laminates, owing to the poor adhesion between the original PEEK fibre and carbon fibre prepreg, as measured in Section 3.1. The Charpy impact strength of the CFRPs was significantly improved upon interleaving original PEEK fibres, as the continuous PEEK fibres were involved in bearing the applied load, and the subsequent PEEK fibre delamination and carbon fibre inter-ply separation through the entire thickness of the laminates (as shown in Figure 12 (b)) resulted in significant energy absorption. The improved PEEK fibre/epoxy adhesion due to the UV-irradiation significantly affected the failure of the impact specimens, i.e. all the carbon fibre plies and PEEK fibres broke into two halves at the fracture point, accompanied by significant inter-ply delamination (two major inter-ply delaminations were observed for the specimen shown in Figure 12 (b)). Further improvements in the Charpy impact strength for the UV-treated PEEK fibres interleaved laminates were attributed to the additional plastic deformation of the thermoplastic fibres and the enhanced stress transfer between the adjacent carbon fibre plies [33, 36, 52], as a result of the improved PEEK fibre/epoxy adhesion. Additionally, the UV-treated PEEK fibres were more

effectively involved in bearing the applied load, and the subsequent pull-out, plastic deformation and breakage of the PEEK fibres (as shown in Figure 12 (b)) consumed a significant amount of energy.

3.5. Mode-I fracture test

Figure 13 shows the R-curves from the DCB tests of the control and interleaved UD and 5H laminates. The last letter of the material code indicates the orientation of the PEEK fibres, i.e. 'L' means the fibres were placed longitudinally to the crack propagation direction, and 'T' is for the transverse direction. A 'flat' R-curve was obtained for the UD control laminate. The 5H control laminate possessed a wave-shaped R-curve owing to the non-uniformity of the local structures (as a result of the weave style of the carbon fibres). However, the overall trend of the R-curve was also essentially 'flat'. Interlaying PEEK fibres to both the UD and 5H laminates resulted in 'rising' R-curve behaviour in all cases, due to the PEEK fibre bridging during the fracture process, as shown in Figure 14. The R-curves of the UD and 5H laminates interleaved by PEEK(Origin)/L fibres exhibited a steadily 'rising' trend over the entire tested region, while those of all the other interleaved laminates became plateaued at some stage. The mode-I crack initiation energy (G_{IC}^{ini}) and crack propagation energy (G_{IC}^{prop}, based on the average values of the plateau region of the R-curves) from the DCB tests are summarised in Table 2. G_{IC}^{ini} and G_{IC}^{prop} of the UD control laminate were measured to be 190 J/m^2 and 185 J/m^2, respectively. The addition of original PEEK fibres notably decreased G_{IC}^{ini} by approximately 50 %, irrespective of the fibre orientation. This was counteracted by applying the UV-irradiation treatment on the PEEK fibres, i.e. G_{IC}^{ini} increased to approximately 240 J/m^2 for both the longitudinally and transversely orientated fibres. Interlaying PEEK fibres significantly increased G_{IC}^{prop} of the UD control laminates, i.e. an increase of 149 %, 293 % and 219 % was measured upon incorporating the PEEK(Origin)/T, PEEK(UV)/L and PEEK(UV)/T interlayers, respectively. Similarly, G_{IC}^{ini} of the control 5H composite considerably decreased by interlaying the non-treated PEEK fibres, and moderately increased upon

adding the UV-treated fibres, as shown in Table 2. However, unlike the UD laminates, interlaying PEEK(Origin)/T fibres to the 5H control laminate resulted in a 8 % decrease in G_{IC}^{prop}, which will be explained later on. The use of UV-irradiated PEEK fibres as interlayers increased G_{IC}^{prop} by 79 % and 24 % for the 5H laminates with longitudinal and transverse fibres, respectively. No values of G_{IC}^{prop} were available for the laminate interleaved by PEEK(Origin)/L fibres, as the fracture toughness kept increasing and went above 1000 J/m^2 for both the UD and 5H laminates. It should be noted that the improvements in G_{IC}^{prop} upon interlaying original PEEK(Origin)/T fibres and the significant and steady 'rising' R-curves by interlaying original PEEK(Origin)/L fibres provided no practical benefit for the fracture performance of the laminates, as it dramatically decreased G_{IC}^{ini} of the laminates. Overall, interlaying longitudinal UV-treated PEEK fibres resulted in the most significant improvements in the mode-I fracture toughness of the UD and 5H laminates.

Figure 15 shows typical SEM images of the fracture surfaces of the control laminates. It is clear that only a small number of delaminated and broken carbon fibres appeared on the fracture surface of the UD control laminate, due to a strong epoxy/carbon fibre adhesion. Hence, limited carbon fibre bridging took place during the fracture of the UD control laminate, resulting in a low fracture energy. In contrast, evidence of significant carbon fibre bridging, that was associated with fibre delamination and breakage, was observed for the 5H control laminates, corresponding to the relatively high fracture energy. The different fracture mechanisms between the UD and 5H control laminates affected the toughening levels of the PEEK fibres. Typical photographs of the fracture surfaces of the DCB specimens are presented in Figure 16. It was found that almost all the PEEK fibres remained on the upper side of the fracture surfaces if the original PEEK fibres were longitudinally placed. Moreover, no evidence of PEEK fibre breakage was observed as they were still in a long and continuous form. This means that the crack propagated interfacially between the PEEK fibres and the carbon fibre plies, that was associated with PEEK fibre debonding from the lower side of the fracture surfaces. In this case, the length of the region containing PEEK fibre bridg-

ing (behind the crack front) continuously increased as the crack propagated. This explains why the R-curves of these laminates show a steadily 'rising' trend up to over 1000 J/m^2, as shown in Figure 13. Cohesive failure inside the interlayers took place for the UD and 5H laminates with UV-treated longitudinal fibres, evidenced by the presence of essentially the same quantity of PEEK fibres on both sides of the fracture surfaces. This clearly indicates an improved PEEK/epoxy adhesion following the UV-treatment. The fracture surfaces of all the transverse fibre interleaved laminates appeared more or less the same, i.e. both sides of the fracture surfaces were covered with numerous PEEK fibres. However, on closer examination, more PEEK fibres were pulled out for the original interleaved specimens than the UV-treated ones, as a result of the lower PEEK/epoxy adhesion. It is obvious that PEEK fibre bridging was the main toughening mechanism in all cases. However, for the 5H laminates, a cohesive failure inside the interlayers was always associated with a reduction of the carbon fibre bridging and delamination, which were the main fracture mechanisms of 5H control lamiantes, as shown in Figure 15 (b). This caused detrimental effects on the toughening efficiency, and explained why the PEEK fibre interlayers were more effective for toughening the UD laminates than the 5H laminates, as shown in Table 2. For example, interlaying original PEEK fibres transversely to the crack propagation direction actually decreased the fracture propagation energy by 8 %.

3.6. Discussion on the state of the art

To date, various materials have been used as interlayers of CFRPs, with carbon nanotubes/nanofibres (CNT/CNFs) and thermoplastic veils being the most prevalent and effective candidates. Neat CNT/CNFs were normally incorporated in CFRPs by either in-situ growing them on the carbon fibres using a chemical vapour deposition method or spraying their solutions on to the carbon fibre fabrics. In general, the toughening performance of neat CNT/CNFs as interlayers is relatively poor, e.g. both Li et al. [53] and Arai et al. [54] reported a maximum improvement of around 25 % for the G_{IC}^{prop} of UD CFRPs upon growing

CNFs on the carbon fibre fabrics. Chaudhry et al. [55] briefly summarised the toughening performance of CNT/CNFs as interlayers of CFRPs, and the maximum increases in G_{IC} were reported to be in the range of 6-98 % (the majority of them were below 50 %), with one outstanding exception, i.e. 348 % in [56], where, however, only the initial values of the R-curves were used. CNT/CNFs hybridised with other materials, such as thermoplastic non-wovens [21] and short carbon fibres [26], were also used as interlayers of CFRPs, and the toughening levels of the hybrid interlayers were normally higher than the neat CNT/CNFs due to the additional contribution of the second phases. It should be noted that, for the interlayers containing CNT/CNFs, an optimal areal density of the interlayers exists, above which the fracture toughness started to drop [26, 54, 57]. It is clear that the toughening performance of longitudinal UV-treated PEEK fibres (used in this work) was notably higher than that of the interlayers consisting of CNF/CNTs. Thermoplastic veils are another group of materials showing excellent toughening performance [11, 58–60] as interlayers of CFRPs. Palazzetti and Zucchelli [11] presented a comprehensive review on the fracture behaviour of CFRPs interleaved with thermoplastic veils, and the maximum improvements in G_{IC} were summarised to be around 300 % [61, 62]. Our previous work [58] revealed that interlaying thermoplastic veils could significantly improve G_{IC} of aerospace-grade CFRPs with different carbon fibre architectures, and an all-round maximum increase of 216 % and 71 % was observed for the same UD and 5H laminates as used in this work, respectively. These values were slightly lower than those of the longitudinal UV-treated PEEK fibres, as shown in Table 2. Noteworthily, the toughening levels of thermoplastic veils varied significantly between different studies, and only some of them are competitive with the longitudinal UV-treated PEEK fibres [11, 59]. Overall, the longitudinal UV-treated PEEK fibres are competitive candidates as interlayers for enhancing G_{IC} of both the UD and 5H laminates, when compared to the other most effective state-of-the-art interlayer materials. It should be emphasised, as noted in Section 2.1, that different composite layups were employed for the fracture test specimens and the remaining mechanical characterisation test specimens (flexural, OHT and Charpy im-

pact tests). For the former, PEEK fibres were only placed at the mid-plane of the laminates (in line with many of the other studies referred to here), while for the latter, PEEK fibres were interlaid between every ply. It is recognised that the fracture properties of laminates containing a single layer are likely to be somewhat different to those containing multiple layers of PEEK fibres, but this was outside the scope of the current study. Regarding impact performance, interlaying longitudinal UV-treated PEEK fibres in between all the plies of the 5H laminate significantly improved its Charpy impact strength by 131 %. A number of studies [29, 33, 36, 37, 52] investigated the Charpy impact strength of CFRPs interleaved with different thermoplastic veils. For example, Beylergil et al. [29, 33] used PA66 non-wovens with different areal densities as interlayers of CFRPs, and reported a maximum increase of 15 % in the Charpy impact strength for an areal density of 17 g/m^2. The increase in the impact strength vanished as the areal density of the PA66 non-woven increased to 50 g/m^2. In another study, Beylergil et al. [37] observed that the Charpy impact strength of a CFRP increased by 11 % upon interlaying polyvinyl-alcohol (PVA) non-wovens. Polyacrylonitrile (PAN) fibres in a non-woven form were also used to interlay CFRPs, and the improvements in the Charpy impact strength were reported to be 15 % and 8 % in the literature [36] and [52], respectively. It is obvious that the increase in the Charpy impact strength of CFRPs upon interlaying longitudinal UV-treated PEEK fibres was one order of magnitude higher than the values reported in these references. To date, the research on the OHT strength of interleaved CFRPs is still very limited. Bilge et al. [63] reported a 9 % increase in the OHT strength of a CFRP upon interlaying a P(St-co-GMA) non-woven mat, which was slightly lower than the value of 12.2 % for interlaying longitudinal UV-treated PEEK fibres. In summary, interlaying UV-treated PEEK fibres is outstanding for enhancing the fracture behaviour and damage tolerance (i.e. OHT strength) of CFRPs, and superior for improving the Charpy impact performance of CFRPs. However, it notably increased the thickness of the laminates and subsequently decreased the flexural strength of the 5H CFRPs by around 29 %, while interlaying thermoplastic veils could result in unchanged or even improved flexural strength

of CFRPs in some cases [33–37].

4. Conclusions

This work studied the effects of adding PEEK fibres on the mechanical, impact and fracture performance of carbon fibre/epoxy laminates. An UV-irradiation technique was employed to activate the surface of the PEEK fibres, aiming to improve the PEEK/epoxy adhesion. The surface analysis results demonstrated more oxidation groups, higher polar surface energy and greater wettability of the PEEK surface due to the UV-irradiation. This considerably improved the PEEK/epoxy adhesion and subsequently increased the ultimate tensile strength of the flatwise tensile joints (two PEEK rods bonded with a layer of carbon fibre prepreg) from 0.6-0.7 MPa to 4.9 MPa for the UD (unidirectional) prepreg and to 7.6 MPa for the 5H (5-harness satin weave) prepreg. The enhanced adhesion significantly improved the toughening performance of the PEEK fibres. Interlaying UV-treated PEEK fibres to the 5H laminates increased the open-hole tensile strength from 378 MPa to 402 MPa, the Charpy impact strength from 80.8 kJ/m^2 to 187.0 kJ/m^2, and the maximum mode-I fracture energy from 185 J/m^2 to 726 J/m^2 for the UD laminates and from 527 J/m^2 to 942 J/m^2 for the 5H laminates. Meanwhile, the flexural strength decreased by 29 % due to the interlaying. However, it should be noted that the maximum load during the flexural test was more or less the same between the interleaved and non-interleaved laminates (725$\pm$47 N and 736$\pm$50 N, respectively), and the drop in the strength was due to the thickness increase. Similarly, a more prominent increase, i.e. from 28 kN to 36 kN, was also observed for the open-hole tensile tests if the load-carrying capacity is considered. Overall, this work demonstrated that the UV-treatment is an easy, low-cost and effective method to improve the adhesion between PEEK and epoxy, and interlaying UV-treated PEEK fibres could simultaneously improve the damage tolerance (open-hole tensile strength), impact performance and fracture toughness of the studied CFRPs, with the load-carrying capacity under flexural bending largely unaffected. Moreover, it highlights the significance of the adhesion between the interlayers and

the laminate matrix to the interlay toughening of fibre reinforced plastics.

Acknowledgements

The authors gratefully acknowledge the financial support of the Irish Composites Centre (IComp). We would also like to thank Bombardier Aerospace (UK) and Zyex (UK) for supplying the carbon fibre fabrics and PEEK fibres employed in this study. Dong Quan received funding from the European Union's Horizon 2020 research and innovation programme under the Marie Skłodowska-Curie grant agreement No. 842467.

References

[1] D. Quan, J. L. Urdaniz, A. Ivankovic, Enhancing mode-I and mode-II fracture toughness of epoxy and carbon fibre reinforced epoxy composites using multi-walled carbon nanotubes, Materials & Design 143 (2018) 81 – 92. doi:10.1016/j.matdes.2018.01.051.

[2] D. Carolan, A. Ivankovic, A. J. Kinloch, S. Sprenger, A. C. Taylor, Toughened carbon fibre-reinforced polymer composites with nanoparticle-modified epoxy matrices, Journal of Materials Science 52 (3) (2017) 1767–1788. doi:10.1007/s10853-016-0468-5.

[3] N. C. Adak, S. Chhetri, T. Kuila, N. C. Murmu, P. Samanta, J. H. Lee, Effects of hydrazine reduced graphene oxide on the inter-laminar fracture toughness of woven carbon fiber/epoxy composite, Composites Part B: Engineering 149 (2018) 22 – 30. doi:10.1016/j.compositesb.2018.05.009.

[4] M. Rafiee, F. Nitzsche, J. Laliberte, S. Hind, F. Robitaille, M. R. Labrosse, Thermal properties of doubly reinforced glass fibre/epoxy composites with graphene nanoplatelets, graphene oxide and reduced-graphene oxide, Composites Part B: Engineering 164 (2019) 1 – 9. doi:10.1016/j.compositesb.2018.11.051.

[5] G. Stegschuster, K. Pingkarawat, B. Wendland, A. P. Mouritz, Experimental determination of the mode I delamination fracture and fatigue properties of thin 3D woven composites, Composites Part A: Applied Science and Manufacturing 84 (2016) 308 – 315. doi:10.1016/j.compositesa.2016.02.008.

[6] S. Yan, X. Zeng, A. Long, Experimental assessment of the mechanical behaviour of 3D woven composite T-joints, Composites Part B: Engineering 154 (2018) 108 – 113. doi:10.1016/j.compositesb.2018.08.007.

[7] F. Pegorin, K. Pingkarawat, S. Daynes, A. P. Mouritz, Influence of z-pin length on the delamination fracture toughness and fatigue resistance of pinned composites, Composites Part B: Engineering 78 (2015) 298 – 307. doi:10.1016/j.compositesb.2015.03.093.

[8] M. Li, P. Chen, B. Kong, T. Peng, Z. Yao, X. Qiu, Influences of thickness ratios of flange and skin of composite T-joints on the reinforcement effect of Z-pin, Composites Part B: Engineering 97 (2016) 216 – 225. doi:10.1016/j.compositesb.2016.05.007.

[9] R. Velmurugan, S. Solaimurugan, Improvements in Mode I interlaminar fracture toughness and in-plane mechanical properties of stitched glass/polyester composites, Composites Science and Technology 67 (1) (2007) 61 – 69. doi:10.1016/j.compscitech.2006.03.032.

[10] D. Quan, S. Flynn, M. Artuso, N. Murphy, C. Rouge, A. Ivankovic, Interlaminar fracture toughness of CFRPs interleaved with stainless steel fibres, Composite Structures 210 (2019) 49 – 56. doi:10.1016/j.compstruct.2018.11.016.

[11] R. Palazzetti, A. Zucchelli, Electrospun nanofibers as reinforcement for composite laminates materials -A review, Composite Structures 182 (2017) 711 – 727. doi:10.1016/j.compstruct.2017.09.021.

[12] A. Nistal, B. G. Falzon, S. C. Hawkins, R. Chitwan, C. Garcia-Diego, F. Rubio, Enhancing the fracture toughness of hierarchical composites through amino/functionalised carbon nanotube webs, Composites Part B: Engineering 165 (2019) 537 – 544. doi:10.1016/j.compositesb.2019.02.001.

[13] D. Quan, C. Mischo, X. Li, G. Scarselli, A. Ivankovi, N. Murphy, Improving the electrical conductivity and fracture toughness of carbon fibre/epoxy composites by interleaving MWCNT-doped thermoplastic veils, Composites Science and Technology 182 (2019) 107775. doi:10.1016/j.compscitech.2019.107775.

[14] Y. Xu, S. V. Hoa, Mechanical properties of carbon fiber reinforced epoxy/clay nanocomposites, Composites Science and Technology 68 (3) (2008) 854 – 861. doi:10.1016/j.compscitech.2007.08.013.

[15] M. R. Nobile, M. Raimondo, K. Lafdi, A. Fierro, S. Rosolia, L. Guadagno, Relationships between nanofiller morphology and viscoelastic properties in CNF/epoxy resins, Polymer Composites 36 (6) (2015) 1152–1160. doi:10.1002/pc.23362.

[16] B. K. Behera, B. P. Dash, Mechanical behavior of 3D woven composites, Materials & Design 67 (2015) 261 – 271. doi:10.1016/j.matdes.2014.11.020.

[17] J. Hoffmann, G. Scharr, Compression properties of composite laminates reinforced with rectangular z-pins, Composites Science and Technology 167 (2018) 463 – 469. doi:10.1016/j.compscitech.2018.08.042.

[18] F. Aymerich, C. Pani, P. Priolo, Damage response of stitched cross-ply laminates under impact loadings, Engineering Fracture Mechanics 74 (4) (2007) 500 – 514. doi:10.1016/j.engfracmech.2006.05.012.

[19] L. Francesconi, F. Aymerich, Effect of Z-pinning on the impact resistance of composite

laminates with different layups, Composites Part A: Applied Science and Manufacturing 114 (2018) 136 – 148. doi:10.1016/j.compositesa.2018.08.013.

[20] L. Daelemans, S. van der Heijden, I. D. Baere, H. Rahier, W. V. Paepegem, K. D. Clerck, Using aligned nanofibres for identifying the toughening micromechanisms in nanofibre interleaved laminates, Composites Science and Technology 124 (2016) 17 – 26. doi:10.1016/j.compscitech.2015.11.021.

[21] N. Zheng, Y. Huang, H.-Y. Liu, J. Gao, Y.-W. Mai, Improvement of interlaminar fracture toughness in carbon fiber/epoxy composites with carbon nanotubes/polysulfone interleaves, Composites Science and Technology 140 (2017) 8 – 15. doi:10.1016/j.compscitech.2016.12.017.

[22] M. Arai, J. ichi Hirokawa, Y. Hanamura, H. Ito, M. Hojo, M. Quaresimin, Characteristic of mode I fatigue crack propagation of CFRP laminates toughened with CNF interlayer, Composites Part B: Engineering 65 (2014) 26 – 33. doi:10.1016/j.compositesb.2014.02.025.

[23] O. Kaynan, Y. Atescan, E. Ozden-Yenigun, H. Cebeci, Mixed mode delamination in carbon nanotube/nanofiber interlayered composites, Composites Part B: Engineering 154 (2018) 186 – 194. doi:10.1016/j.compositesb.2018.07.032.

[24] H. Ning, J. Li, N. Hu, C. Yan, Y. Liu, L. Wu, F. Liu, J. Zhang, Interlaminar mechanical properties of carbon fiber reinforced plastic laminates modified with graphene oxide interleaf, Carbon 91 (2015) 224 – 233. doi:10.1016/j.carbon.2015.04.054.

[25] X. Du, H. Zhou, W. Sun, H.-Y. Liu, G. Zhou, H. Zhou, Y.-W. Mai, Graphene/epoxy interleaves for delamination toughening and monitoring of crack damage in carbon fibre/epoxy composite laminates, Composites Science and Technology 140 (2017) 123 – 133. doi:10.1016/j.compscitech.2016.12.028.

[26] H. Zhou, X. Du, H.-Y. Liu, H. Zhou, Y. Zhang, Y.-W. Mai, Delamination toughening of carbon fiber/epoxy laminates by hierarchical carbon nanotube-short carbon fiber interleaves, Composites Science and Technology 140 (2017) 46 – 53. doi:10.1016/j.compscitech.2016.12.018.

[27] B. Wang, Y. Bai, X. Hu, P. Lu, Enhanced epoxy adhesion between steel plates by surface treatment and CNT/short-fibre reinforcement, Composites Science and Technology 127 (2016) 149 – 157. doi:10.1016/j.compscitech.2016.03.008.

[28] T. Brugo, R. Palazzetti, The effect of thickness of Nylon 6,6 nanofibrous mat on Modes I-II fracture mechanics of UD and woven composite laminates, Composite Structures 154 (2016) 172 – 178. doi:10.1016/j.compstruct.2016.07.034.

[29] B. Beylergil, M. Tanoglu, E. Aktas, Effect of polyamide-6,6 (PA 66) nonwoven veils on the mechanical performance of carbon fiber/epoxy composites, Composite Structures 194 (2018) 21 – 35. doi:10.1016/j.compstruct.2018.03.097.

[30] N. H. Nash, T. M. Young, P. T. McGrail, W. F. Stanley, Inclusion of a thermoplastic phase to improve impact and post-impact performances of carbon fibre reinforced thermosetting composites - A review, Materials & Design 85 (2015) 582 – 597. doi:10.1016/j.matdes.2015.07.001.

[31] S. Hamer, H. Leibovich, A. Green, R. Intrater, R. Avrahami, E. Zussman, A. Siegmann, D. Sherman, Mode-I interlaminar fracture toughness of nylon 66 nanofibrilmat interleaved carbon/epoxy laminates, Polymer Composites 32 (11) (2011) 1781–1789. doi:10.1002/pc.21210.

[32] Y. Zhao, T. Xu, X. Ma, M. Xi, D. R. Salem, H. Fong, Hybrid multi-scale epoxy composites containing conventional glass microfibers and electrospun glass nanofibers with improved mechanical properties, Journal of Applied Polymer Science 132 (44) (2015). doi:10.1002/app.42731.

[33] B. Beylergil, M. Tanoglu, E. Aktas, Enhancement of interlaminar fracture toughness of carbon fiber/epoxy composites using polyamide-6,6 electrospun nanofibers, Journal of Applied Polymer Science 134 (35) (2017) 45244. doi:10.1002/app.45244.

[34] D. W. Wong, L. Lin, P. T. McGrail, T. Peijs, P. J. Hogg, Improved fracture toughness of carbon fibre/epoxy composite laminates using dissolvable thermoplastic fibres, Composites Part A: Applied Science and Manufacturing 41 (6) (2010) 759 – 767. doi:10.1016/j.compositesa.2010.02.008.

[35] J. Herwan, E. Al-Bahkali, K. A. Khalil, M. Souli, Load bearing enhancement of pin joined composite laminates using electrospun polyacrylonitrile nanofiber mats, Arabian Journal of Chemistry 9 (2) (2016) 262 – 268. doi:10.1016/j.arabjc.2015.03.019.

[36] L. M. K. Molnar, E. Kostakova, The effect of needleless electrospun nanofibrous interleaves on mechanical properties of carbon fabrics/epoxy laminates, eXPRESS Polymer Letters 8 (1) (2014) 62–72. doi:10.3144/expresspolymlett.2014.8.

[37] B. Beylergil, M. Tanoglu, E. Aktas, Modification of carbon fibre/epoxy composites by polyvinyl alcohol (PVA) based electrospun nanofibres, Advanced Composites Letters 25 (3) (2016) 69–76. doi:10.1177/096369351602500303.

[38] K. O'Donovan, D. Ray, M. A. McCarthy, Toughening effects of interleaved nylon veils on glass fabric/low-styrene-emission unsaturated polyester resin composites, Journal of Applied Polymer Science 132 (7) (2015) 41462. doi:10.1002/app.41462.

[39] J. Zhang, T. Yang, T. Lin, C. H. Wang, Phase morphology of nanofibre interlayers: Critical factor for toughening carbon/epoxy composites, Composites Science and Technology 72 (2) (2012) 256 – 262. doi:10.1016/j.compscitech.2011.11.010.

[40] V. A. Ramirez, P. J. Hogg, W. W. Sampson, The influence of the nonwoven veil architectures on interlaminar fracture toughness of interleaved composites, Composites Science and Technology 110 (2015) 103 – 110. doi:10.1016/j.compscitech.2015.01.016.

[41] UV Power Puck from EIT Inc., USA, Last Accessed: 27th November 2019.
URL https://www.eit.com/sites/default/files/instruments/100200%20PP2HU_revB.pdf

[42] ISO 14125:1998, Fibre-reinforced plastic composites -Determination of flexural properties, International Organization for Standardization (1998).

[43] ASTM Standard D5766/D5766M, Standard Test Method for Open-Hole Tensile Strength of Polymer Matrix Composite Laminates, ASTM International (2018).

[44] ISO 179-1:2010, Plastics-Determination of Charpy impact properties-Part 1: Non-instrumented impact test, International Organization for Standardization (2010).

[45] BS ISO 15024:2001, Fibre-reinforced plastic composites Determination of mode I interlaminar fracture toughness, G_{IC} for unidirectionally reinforced materials, International Organization for Standardization (2001).

[46] G. K. A. Kodokian, A. J. Kinloch, The adhesive fracture energy of bonded thermoplastic fibre-composites, The Journal of Adhesion 29 (1-4) (1989) 193–218. doi:10.1080/00218468908026487.

[47] A. J. Kinloch, G. K. A. Kodokian, J. F. Watts, The adhesion of thermoplastic fibre composites, Philosophical Transactions of the Royal Society of London. Series A: Physical and Engineering Sciences 338 (1649) (1992) 83–112. doi:10.1098/rsta.1992.0004.

[48] I. Mathieson, R. H. Bradley, Improved adhesion to polymers by UV/ozone surface oxidation, International Journal of Adhesion and Adhesives 16 (1) (1996) 29 – 31. doi:10.1016/0143-7496(96)88482-X.

[49] L. Liu, H. Zhang, Y. Zhou, Quasi-static mechanical response and corresponding analytical model of laminates incorporating with nanoweb interlayers, Composite Structures 111 (2014) 436 – 445. doi:10.1016/j.compstruct.2014.01.021.

[50] B. Green, M. Wisnom, S. Hallett, An experimental investigation into the tensile strength scaling of notched composites, Composites Part A: Applied Science and Manufacturing 38 (3) (2007) 867 – 878. doi:10.1016/j.compositesa.2006.07.008.

[51] B. Chen, T. Tay, P. Baiz, S. Pinho, Numerical analysis of size effects on open-hole tensile composite laminates, Composites Part A: Applied Science and Manufacturing 47 (2013) 52 – 62. doi:10.1016/j.compositesa.2012.12.001.

[52] R. E. Neisiany, S. N. Khorasani, M. Naeimirad, J. K. Y. Lee, S. Ramakrishna, Improving mechanical properties of carbon/epoxy composite by incorporating functionalized electrospun polyacrylonitrile nanofibers, Macromolecular Materials and Engineering 302 (5) (2017) 1600551. doi:10.1002/mame.201600551.

[53] Y. Li, N. Hori, M. Arai, N. Hu, Y. Liu, H. Fukunaga, Improvement of interlaminar mechanical properties of CFRP laminates using VGCF, Composites Part A: Applied Science and Manufacturing 40 (12) (2009) 2004 – 2012. doi:10.1016/j.compositesa.2009.09.002.

[54] M. Arai, Y. Noro, K. ichi Sugimoto, M. Endo, Mode I and mode II interlaminar fracture toughness of CFRP laminates toughened by carbon nanofiber interlayer, Composites Science and Technology 68 (2) (2008) 516 – 525. doi:10.1016/j.compscitech.2007.06.007.

[55] M. S. Chaudhry, A. Czekanski, Z. H. Zhu, Characterization of carbon nanotube enhanced interlaminar fracture toughness of woven carbon fiber reinforced polymer composites, International Journal of Mechanical Sciences 131-132 (2017) 480 – 489. doi:10.1016/j.ijmecsci.2017.06.016.

[56] V. P. Veedu, A. Cao, X. Li, K. Ma, C. Soldano, S. Kar, P. M. Ajayan, M. N. Ghasemi-Nejhad, Multifunctional composites using reinforced laminae with carbon-nanotube forests, Nature Materials 5 (2006) 457 – 462. doi:10.1038/nmat1650.

[57] N. Hu, Y. Li, T. Nakamura, T. Katsumata, T. Koshikawa, M. Arai, Reinforcement effects of MWCNT and VGCF in bulk composites and interlayer of CFRP laminates, Composites Part B: Engineering 43 (1) (2012) 3 – 9. doi:10.1016/j.compositesb.2011.04.022.

[58] D. Quan, F. Bologna, G. Scarselli, A. Ivankovic, N. Murphy, Interlaminar fracture toughness of aerospace-grade carbon fibre reinforced plastics interleaved with thermoplastic veils, Composites Part A: Applied Science and Manufacturing 128 (2020) 105642. doi:10.1016/j.compositesa.2019.105642.

[59] D. Quan, C. Mischo, L. Binsfeld, A. Ivankovic, N. Murphy, Fracture behaviour of carbon fibre/epoxy composites interleaved by MWCNT- and graphene nanoplatelet-doped thermoplastic veils, Composite Structures (2019) 111767doi:10.1016/j.compstruct.2019.111767.

[60] D. Quan, F. Bologna, G. Scarselli, A. Ivankovic, N. Murphy, Mode-II fracture behaviour of aerospace-grade carbon fibre/epoxy composites interleaved with thermoplastic veils, Composites Science and Technology (2020) 108065doi:10.1016/j.compscitech.2020.108065.

[61] H. Zhang, A. Bharti, Z. Li, S. Du, E. Bilotti, T. Peijs, Localized toughening of carbon/epoxy laminates using dissolvable thermoplastic interleaves and electrospun fi-

bres, Composites Part A: Applied Science and Manufacturing 79 (2015) 116 – 126. doi:10.1016/j.compositesa.2015.09.024.

[62] G. Li, P. Li, Y. Yu, X. Jia, S. Zhang, X. Yang, S. Ryu, Novel carbon fiber/epoxy composite toughened by electrospun polysulfone nanofibers, Materials Letters 62 (3) (2008) 511 – 514. doi:10.1016/j.matlet.2007.05.080.

[63] K. Bilge, S. Venkataraman, Y. Menceloglu, M. Papila, Global and local nanofibrous interlayer toughened composites for higher in-plane strength, Composites Part A: Applied Science and Manufacturing 58 (2014) 73 – 76. doi:10.1016/j.compositesa.2013.12.001.

Figures

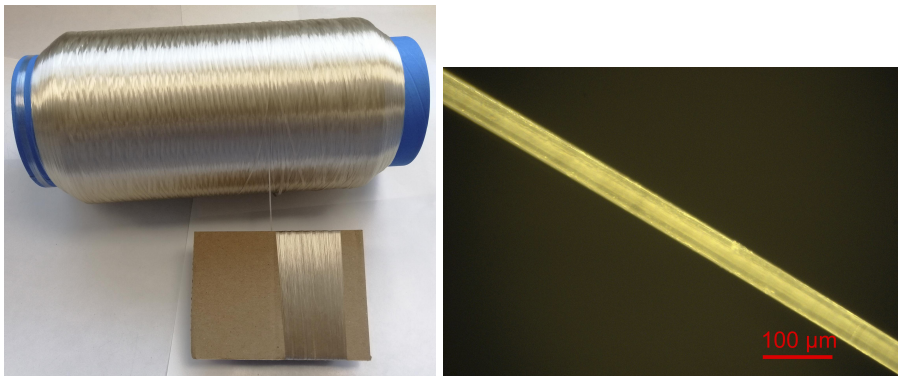

(a) (b)

Figure 1: (a) The PEEK fibre yarn and a cardboard sheet wound with PEEK fibres; and (b) A typical microscopy image of a PEEK fibre

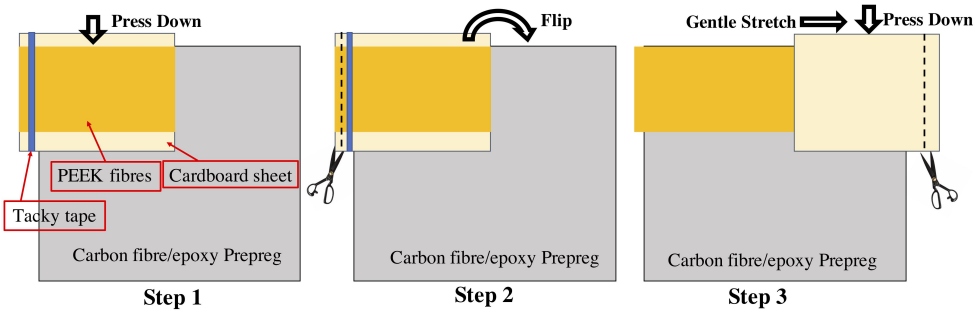

Figure 2: Schematic of the placement of the PEEK fibre interlayers onto the prepregs.

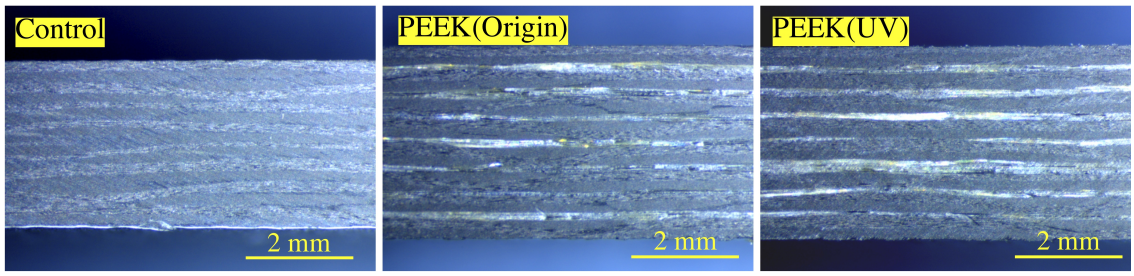

Figure 3: Representative optical microscopy images of the laminates consisting of 8 plies of 5H laminates with and without PEEK fibre interleaves (side-view).

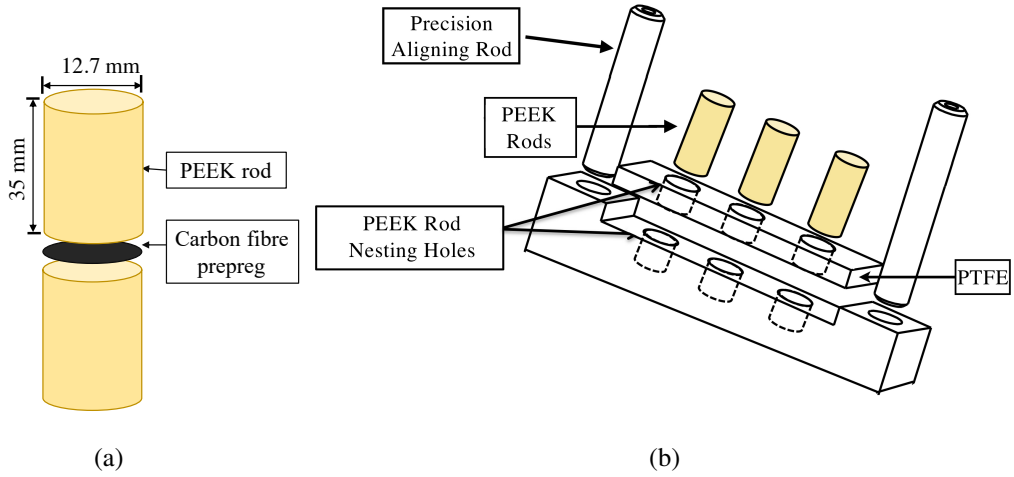

Figure 4: Schematics of (a) the flatwise tensile specimens; and (b) the lower section of the bonding rig.

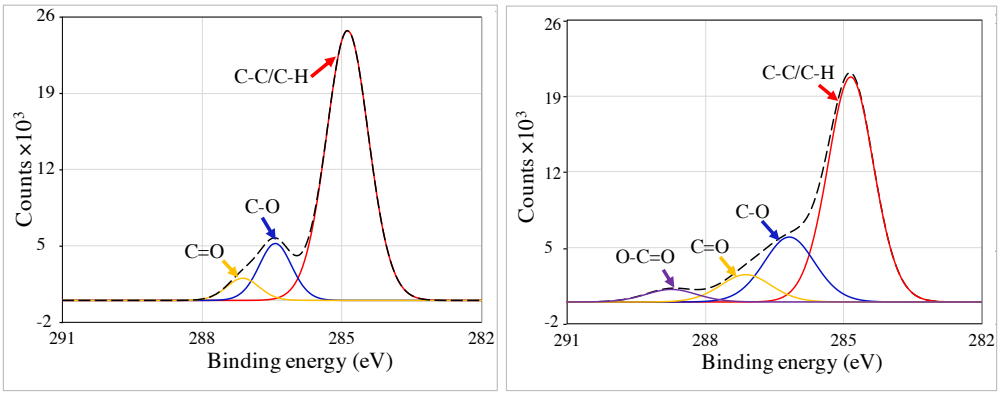

(a) PEEK(Origin) (b) PEEK(UV)

Figure 5: Typical results of a narrow XPS scan of the carbon peak for: (a) the control PEEK; and (b) the UV-treated PEEK.

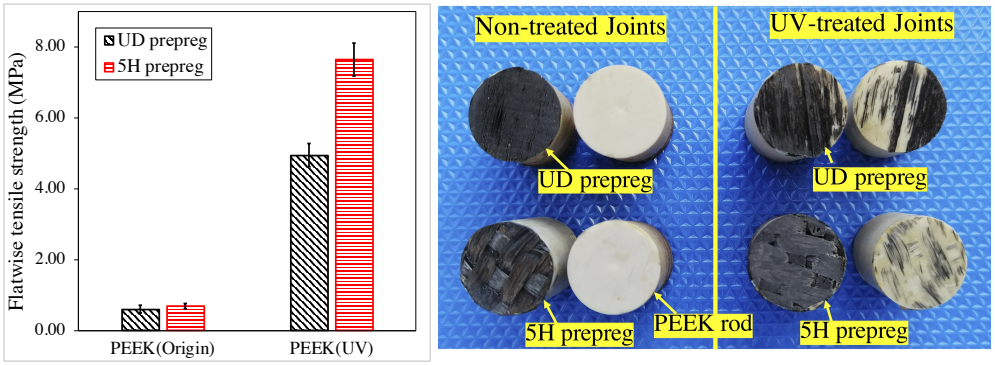

(a) Flatwise tensile strength (b) Failure surface

Figure 6: (a) Flatwise tensile strength of the PEEK joints bonded by the carbon fibre prepreg; and (b) failure surfaces of the flatwise tensile specimens.

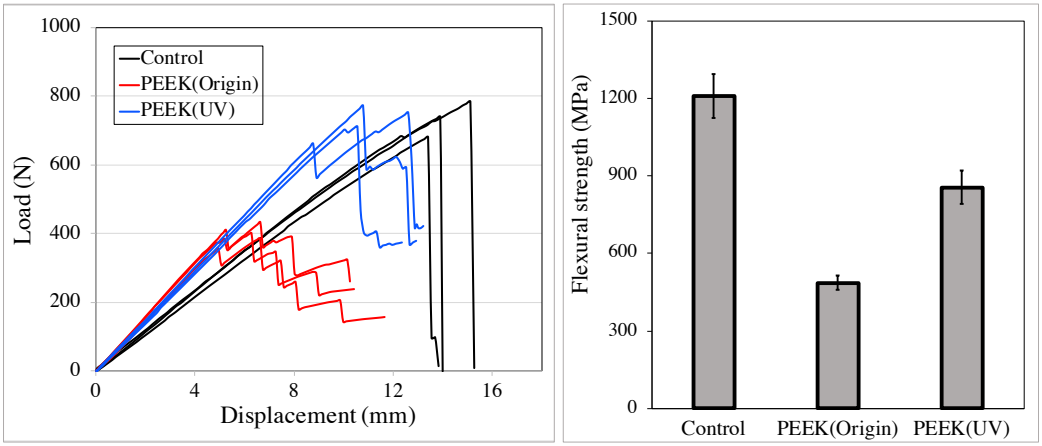

(a) Load-displacement curves (b) Flexural strength

Figure 7: The results of the three-point bend flexural tests; (a) load versus displacement curves, and (b) flexural strength.

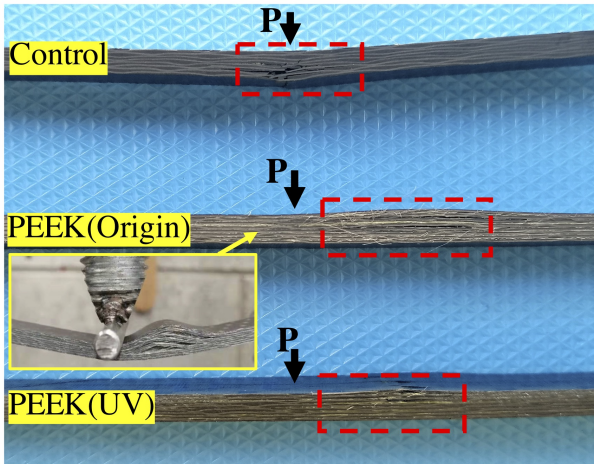

(a)

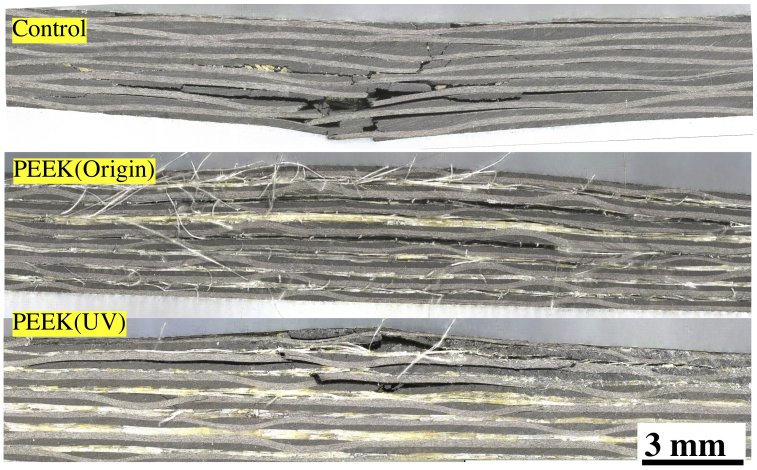

(b)

Figure 8: Failure mode of the flexural specimens: (a) photos of the fractured specimens and (b) laser microscopy images of the damage region. The red dashed boxes in (a) indicate the damage regions, corresponding to the imaged regions in (b).

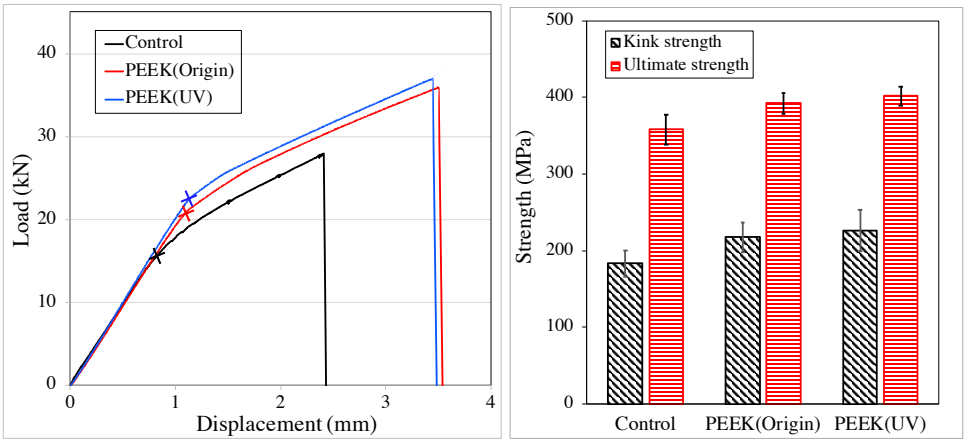

(a) Load-displacement curves (b) Kink strength and ultimate strength

Figure 9: (a) the load versus displacement curves and (b) the strength at the kink and the failure point from the OHT tests. The cross points in (a) indicate the initiation of the damage or 'kink'.

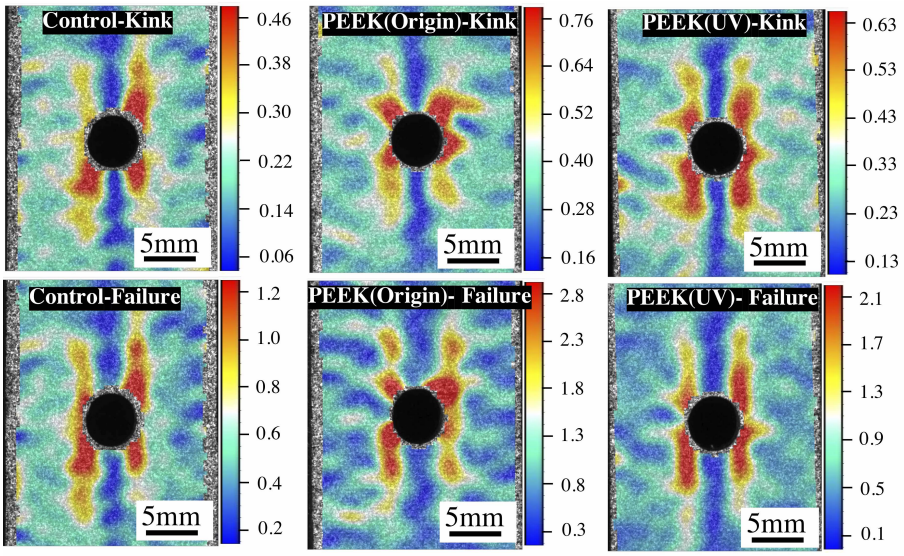

Figure 10: Full-field von Mises equivalent strain (ε_{vM}) contours of the surface of the OHT specimens at the time of the kink and the final failure.

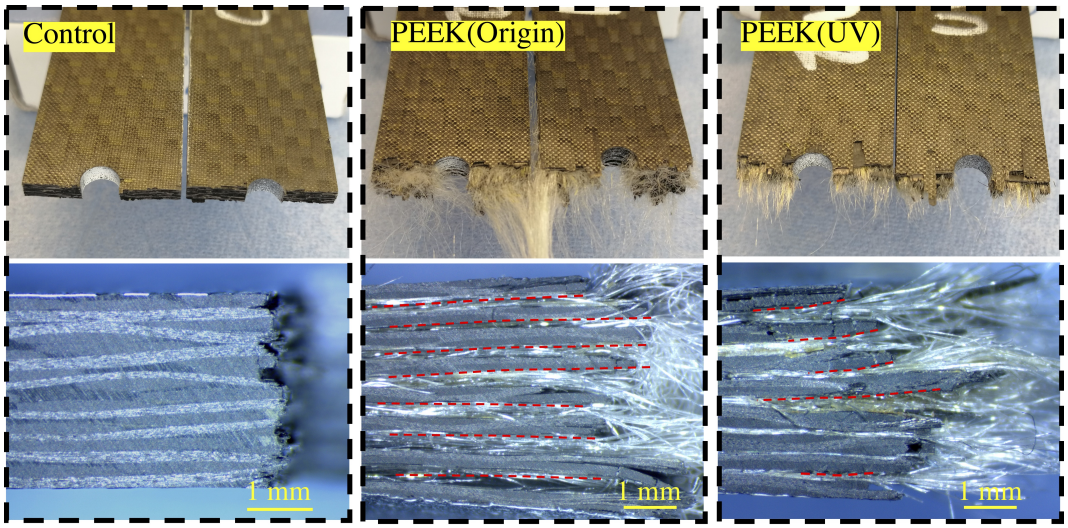

Figure 11: Typical photographs of the tested OHT specimens. The bottom pictures are side-view images focusing on the vicinity of the fracture plane. The red dashed lines indicate the inter-ply separation/delamination.

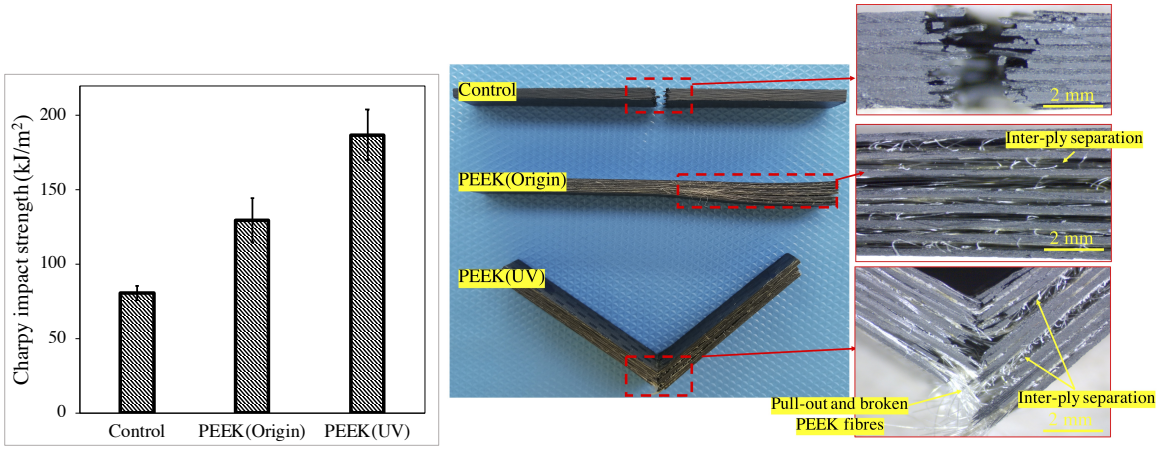

(a) Charpy impact strength (b) Typical images of the impacted specimens

Figure 12: (a) Charpy impact strengths of the laminates, and (b) typical images of the tested Charpy impact specimens.

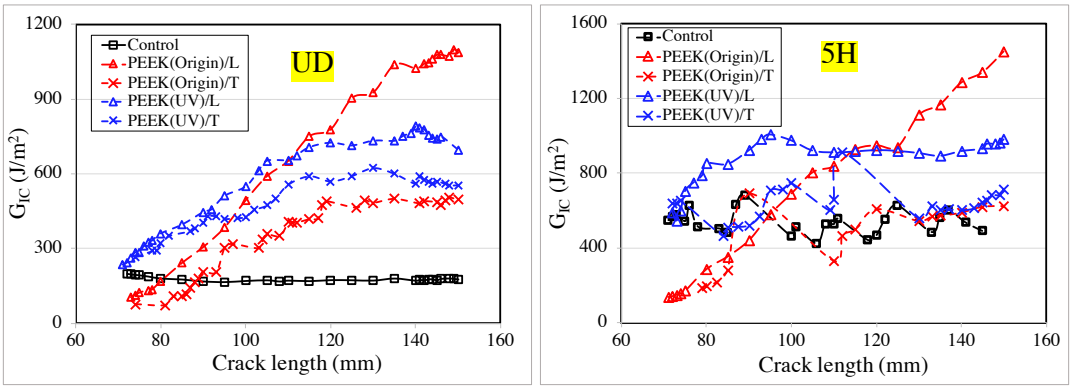

(a) UD laminates (b) 5H laminates

Figure 13: R-curves from the DCB tests of the control and interleaved laminates.

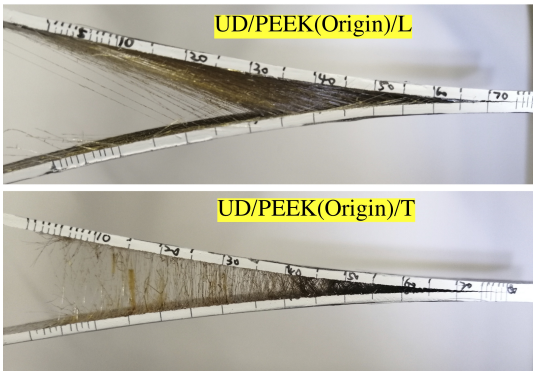

Figure 14: PEEK fibre bridging during the mode-I fracture tests.

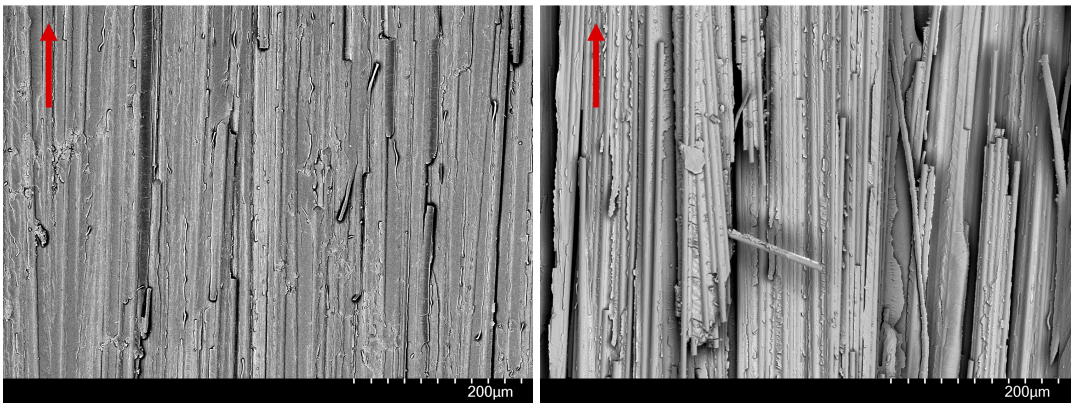

(a) UD control (b) 5H control

Figure 15: Typical SEM images of the control laminates. The red arrows indicate the crack propagating direction.

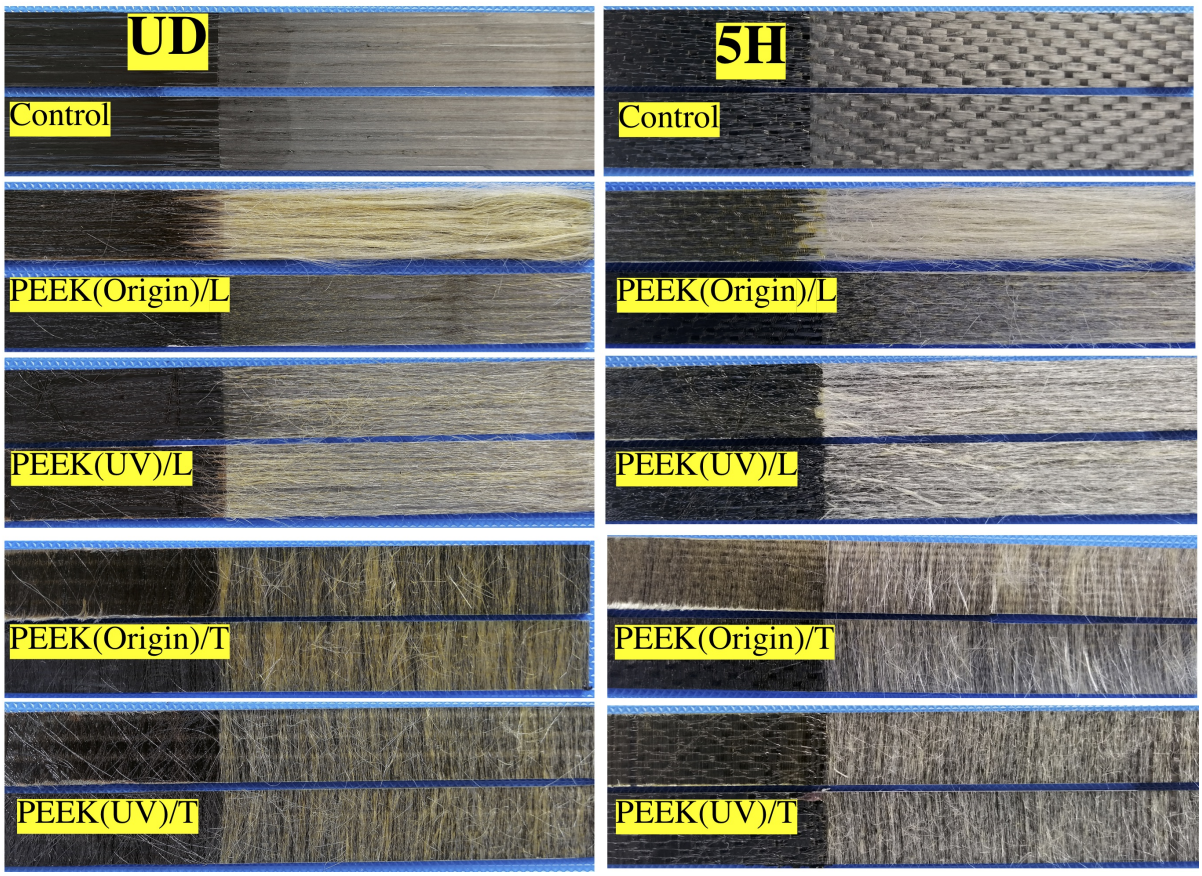

Figure 16: Typical photographs of the fracture surfaces of different laminates. The upper and lower fracture surfaces are from the same specimens in each case.

Tables

Table 1: The amount of carbon and oxygen elements, surface free energies (γ) together with corresponding surface disperse force (γ_d) and polar force (γ_s) and water contact angles (θ) of the PEEK surfaces.

TPCs	C (%)	O (%)	γ (mN/m)	γ_d (mN/m)	γ_s (mN/m)	θ ($^\circ$)
PEEK (Origin)	82.89	14.55	50.03	48.32	1.71	81.49
PEEK (UV)	73.44	22.02	50.77	44.15	6.61	69.09

Table 2: Results of the DCB tests. The values in the brackets indicate percentage increases over the values of the control specimens.

Materials	G_{IC}^{ini} (J/m^2)	G_{IC}^{prop} (J/m^2)
UD/Control	190$\pm$23	185$\pm$15
UD/PEEK(Origin)/L	89$\pm$17 (-53 %)	$*$
UD/PEEK(Origin)/T	100$\pm$21 (-47 %)	461$\pm$25 (149 %)
UD/PEEK(UV)/L	237$\pm$22 (25 %)	726$\pm$82 (293 %)
UD/PEEK(UV)/T	247$\pm$27 (30 %)	591$\pm$15 (219 %)
5H/Control	502$\pm$40	527$\pm$32
5H/PEEK(Origin)/L	140$\pm$9 (-72 %)	$*$
5H/PEEK(Origin)/T	208$\pm$52 (-59 %)	484$\pm$33 (-8 %)
5H/PEEK(UV)/L	585$\pm$36 (17 %)	942$\pm$68 (79 %)
5H/PEEK(UV)/T	666$\pm$52 (33 %)	656$\pm$58 (24 %)